BULLETIN DE L'ASSOCIATION MINERALOGIQUE DU CANADA

THE CANADIAN MINERALOGIST

JOURNAL OF THE MINERALOGICAL ASSOCIATION OF CANADA

Volume 27 March 1989 Part 1

Canadian Mineralogist
Vol. 27, pp. 1-14 (1989)

ON MODELS AND MODELING[1]

HUGH J. GREENWOOD
Department of Geological Sciences, The University of British Columbia,
6339 Stores Road, Vancouver, British Columbia V6T 2B4

ABSTRACT

The word 'model' appears so frequently in the geological literature that its meaning is in danger of being degraded to indicate little more than a speculative hunch about how some part of nature may have functioned. This paper is a plea to reserve the word 'model' to well-constrained logical propositions with *necessary, testable* consequences. Some examples of thermodynamic modeling are presented by way of illustration.

Keywords: model, predictions, thermodynamic model, petrology, basalt–eclogite transition.

SOMMAIRE

Le mot "modèle" est utilisé si couramment dans la littérature géologique qu'il risque de devenir ni plus ni moins que l'expression d'un soupçon préliminaire du mode de fonctionnement d'un phénomène naturel quelconque. Cet article se veut un plaidoyer en faveur d'une restriction du mot "modèle" pour exprimer une proposition logique bien encadrée, ayant des conséquences nécessaires et testables. Quelques exemples relevés parmi les modèles thermodynamiques illustrent le concept.

(Traduit par la Rédaction)

Mots-clés: modèle, prédictions, modèle thermodynamique, pétrologie, transition de basalte à éclogite.

INTRODUCTION

This presentation might equally well have been entitled "Borrowed Flowers", after Montaigne ("Comme quelqu'un pourrait dire de moi que j'ai un amas de fleurs étrangères, n'y ayant fourni du mien que le filet à les lier")[2] because most of what I offer in what follows is based on the work of the excellent students and colleagues with whom I have been so lucky to associate. Most of what I show is theirs, except for any errors I might introduce.

The word 'model' appears with increasing frequency and decreasing discrimination in the jargon of geology and petrology. Indeed, I counted 93 occurrences of the word in this year's (1988) GAC–MAC abstracts. About half of these occurrences represent an uncomfortably close approach to what I refer to as 'Cloud - 9 models', where there is more speculation than prediction. As is argued in the following paragraphs, we should reserve the word 'model' for well-constrained logical propositions, not necessarily mathematical, that have *necessary* and *testable* consequences, and avoid the use of the word if we are merely constructing a scenario of possibilities.

WHAT IS A MODEL?

Ask the man on the street what he thinks a model is, and you will probably get a variety of answers, ranging from "a human clothes-horse", through "role model", "a statue", or "a toy boat". Ask a geologist the same question, and you are likely to

---

[1] Presidential Address, Mineralogical Association of Canada, May 1988, St. John's, Newfoundland.

[2] "And one might therefore say of me that I have but gathered other people's flowers, and contributed only the thread that ties them together".

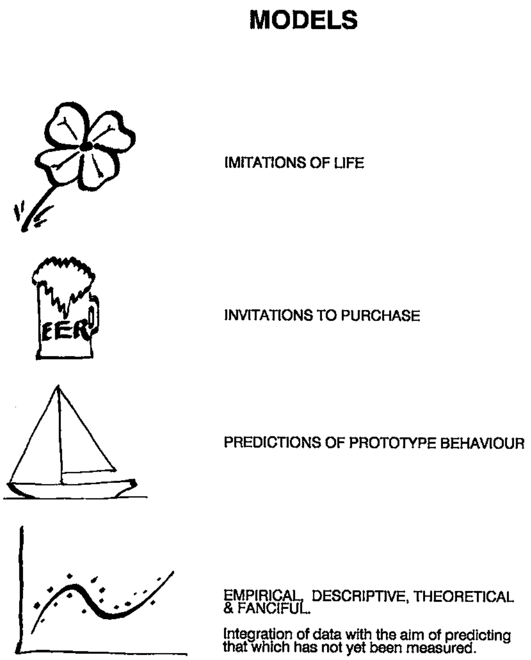

FIG. 1. Some varieties of models.

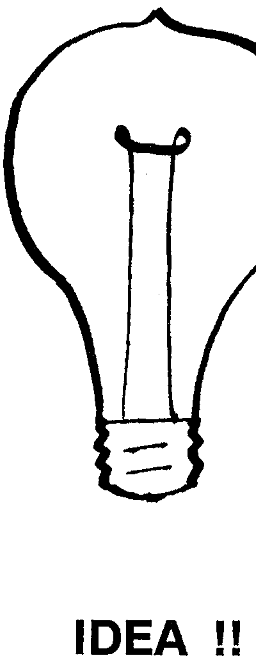

FIG. 2. The basic 'conceptual model'.

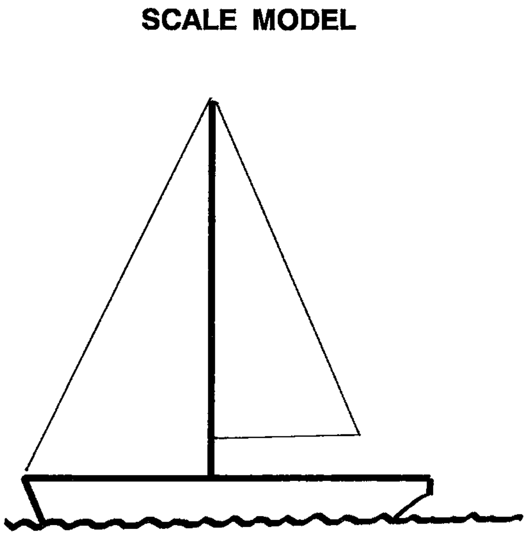

FIG. 3. The scale model, subject to scaling laws.

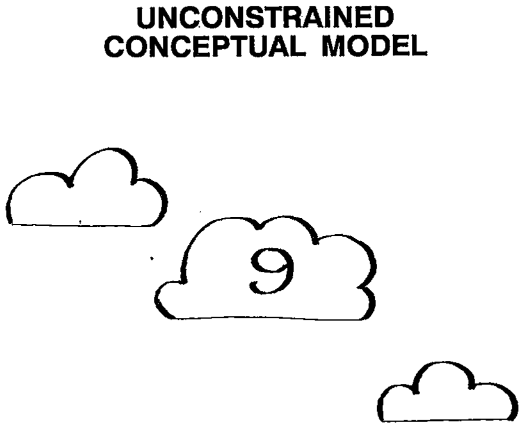

FIG. 4. The 'cloud-9' unconstrained model.

hear words like "porphyry copper model", "facies model", "crystal-structure model", "morphological model", and "heat-flow model". Clearly, there are many kinds of models, some of which are illustrated in Figure 1. Some models are meant to be an imitation of life, some are designed to induce us to buy a product. Some are physical models made to emulate the behavior of a prototype, and some are empirical or theoretical descriptions of the behavior of some system or other.

Scientific models begin with an idea (Fig. 2). The idea is a 'conceptual model', and it may survive if it is well-constrained by observation and if it has logical consequences not yet observed but required by the concept. Testing the model against new observations will either support the model or force its rejection. A model that has no predicted testable consequences is unverifiable and, if not useless, it is, at best, sterile.

Some very useful models are *scale models*, in which one builds a physical model of a real system, commonly on a reduced scale, with the objective of predicting the behavior of the prototype (Fig. 3). Among such models are scale models of hydrodynamic systems, such as boats, flumes, and rivers, where rigorous scaling laws apply. Commonly it is impossible to scale with complete dimensional similarity, with the result that some, but not all, of the prototype behavior will be accurately simulated. For example, in the tank testing of model ships, proper scaling of dimensions and velocity may require scaling of viscosity and density to a range where there are no materials available for the experiment, with the result that some important features may not be simulated.

We should, perhaps, remark on the archetypical *'conceptual model'* or 'Cloud-9 model' (Fig. 4), in which we express some vague notion that has few, if any, testable consequences. I suggest that there are too many such 'models' in our science, and that they do not deserve the appellation 'model'. It is their lack of *necessary* consequences that damns them. Indeed, all too often the word is used to add the illusion of profound thought to a weak or preposterous speculation. "Scenario" might be a better word.

DESCRIPTIVE MODELS

There are many descriptive models of great value in which observations are summarized, organized, and presented. Figure 5 illustrates a 'Cloud-9' descriptive 'model' in which totally inadequate data (from a single drill-hole) are used to imply structures and processes for which there is no evidence. The hypothetical structure is testable, to be sure, by further drilling, but the hypothesis is unfounded, and there is no real prediction. Figure 6 illustrates another type of descriptive model, the empirical descriptive model, in which data are described by some function or other, unconstrained by theory or necessary boundary conditions. Such models can be made to describe the data with as much detail as is desired, and can have powerful predictive capabilities *within the range of the data* where the predicted value of a new datum is known to within a definite statistical certainty. However, unconstrained empirical models commonly perform very badly when used to extrapolate outside the range of the primary data. A stronger kind of descriptive empirical model is the constrained descriptive model, illustrated in Figure 7, in which a functional form derived from theory is fitted to the data. Boundary conditions imposed by theoretical considerations force the function to behave well and to serve the predictive goal outside of the range of the data, provided, of course, that the theoretical framework is correct. In Figure 7, the conceptual model is one of internal homogeneous equilibrium, which requires that the first derivatives of $G(x)$ approach infinity at $x=1,0$, and that the second derivative be positive everywhere in the range $x=1$ to 0.

Some excellent models are not directly deterministic, but stochastic or probabilistic. Figure 8 illustrates a likelihood map, where the probability of encountering some value of a system property is dictated by statistical theory, with the likelihood being a direct consequence of the model.

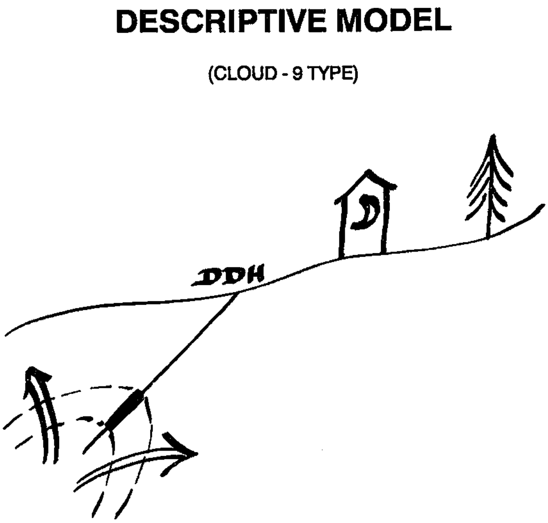

FIG. 5. A descriptive cloud-9 model.

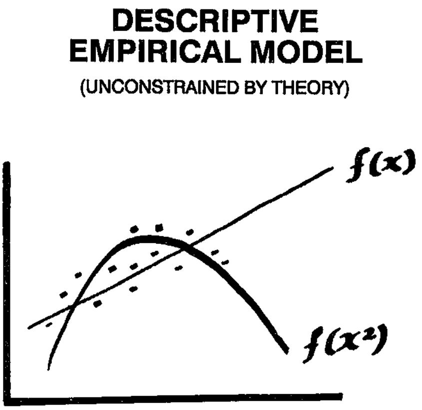

FIG. 6. A descriptive empirical model without a constraining theoretical basis or boundary conditions.

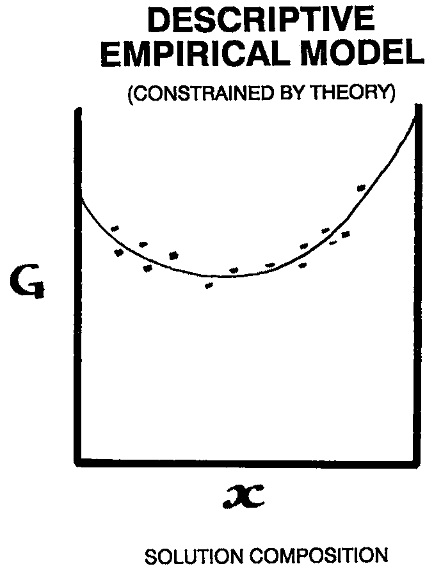

FIG. 7. A descriptive empirical model with theoretical boundary conditions imposed.

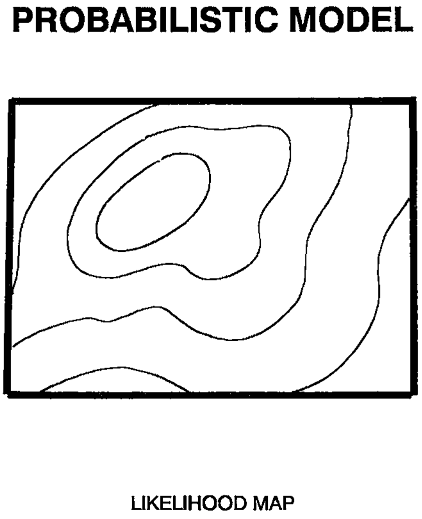

FIG. 8. Sketch of a probabilistic model.

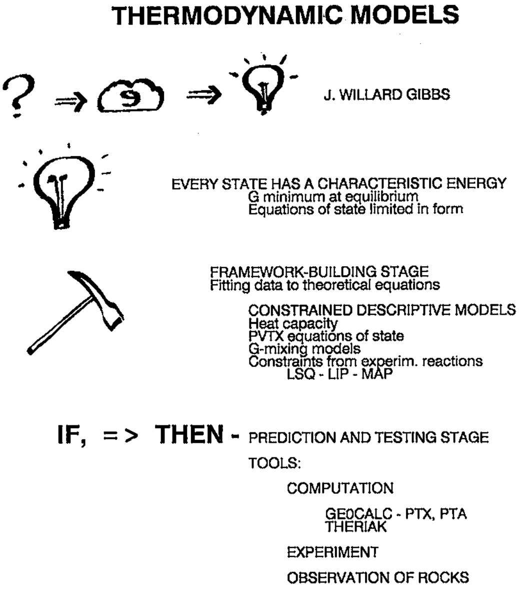

FIG. 9. The growth stages of a model.

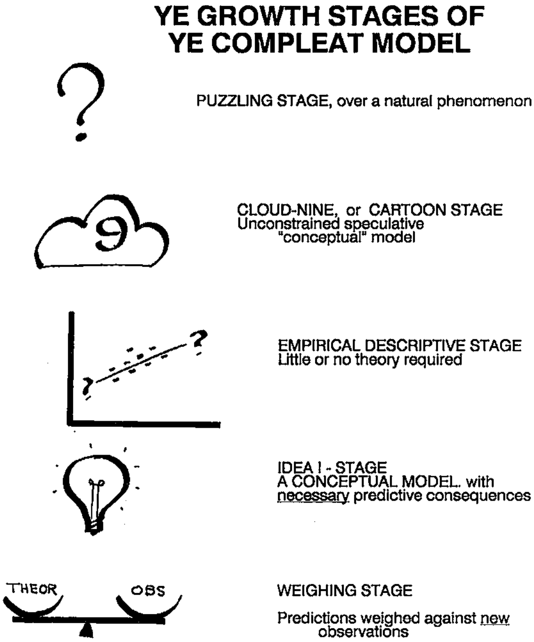

FIG. 10. Evolution of thermodynamic modeling.

Good models go through evolutionary stages, some of which are illustrated in Figure 9. In general, we start with a puzzling situation and begin making unconstrained or 'cloud-9' models about it. In science, these are quickly followed by careful observation and an empirical, descriptive stage. We answer the question, "what is it like, in detail?". Somewhere about this stage a conceptual model is born, which, if it is to be useful, will have the form, "If my model is correct, *then* the following new observations could be made and should have the following values". The next stage involves making the new observations and weighing them against their predicted values. From this point the process is recursive, with the model being refined and new data added until the model seems to predict with satisfactory certainty or until it is abandoned. In what follows, I shall use thermodynamic modeling as an example of a mature conceptual model with abundant data, and which has predictive capabilities many thousands of times more extensive than the primary data might suggest. For example, the databases of Berman *et al.* (1985) and Berman (1988) represent 70 phases and 11 components, which can be used to infer and calculate some 10^{10} different equilibria. A lucrative field indeed for testing and refinement!

THERMODYNAMIC MODELS

Figure 10 illustrates the evolution of thermodynamic modeling, marking the beginning of our current conceptual model with the work of J. Willard Gibbs (1876), which assumes that every definite state of a well-defined chemical system is characterized by a unique value of its internal energy. Gibbs showed that there are rigorous consequences to this assumption, which are now expressed in the familiar equations of thermodynamics. These equations provide the functional form that must be used in theoretically constrained thermodynamic models of chemical systems, including mineralogical systems. In this effort we are now in the recursive stage, moving back and forth between theoretically constrained models of the thermodynamic properties of minerals and the predicted consequences in the form of computed equilibria that must reflect the underlying data and that should, optimistically, reflect the processes that lead to the formation of the same minerals in the rocks of the earth. As an example of the predict-test-predict-test cycle, there follows an application to the study of eclogites using the data of Berman (1988), and algorithms due to deCapitani & Brown (1987), Perkins *et al.* (1986), and Brown *et al.* (1988).

A basalt - eclogite example

We shall now examine briefly this garland of other people's flowers. For this we shall start by applying the approach of minimization of free energy to a bulk chemical system resembling basalt, and observe how we would predict its mineralogy to change with changes in pressure. The computations were performed using the program "THERIAK" (deCapitani & Brown 1987), which finds, by successive minimizations of free energy, the phase assemblage having the lowest free energy for that bulk composition. THERIAK is a particularly powerful program; besides being quite fast and efficient, it accepts solution models of all kinds for all phases considered, including gas, liquid, and solid. Within the limits of available data, therefore, it is possible to perform a simulation as complete as we desire. The result of a typical calculation gives the name of the stable phases, their composition if they are solid solutions, their modal proportions, and the activities of every other phase or species considered in the system. It is thus easy to see which other phases are close to saturation in the system even if they do not form part of the stable mode.

The basalt chosen for this exercise in modeling is the alkali olivine basalt used in experiments by Green & Ringwood (1967) and quoted by Ringwood (1975, p. 14). Table 1 gives the composition of the natural basalt and the simplified versions of it used for the thermodynamic modeling. Figure 11 shows the variations in modal mineralogy of this alkali olivine

TABLE 1. CHEMICAL COMPOSITIONS OF BASALT AND BASALT MODELS

		1	2	3	4
SiO_2	wt.%	45.4	45.4	44.0	44.0
TiO_2		2.5	.0	.0	.0
Al_2O_3		14.7	14.7	16.8	16.8
Fe_2O_3		1.9	.0	.0	.0
FeO		12.4	12.4	10.0	.0
MnO		0.2	.0	.0	.0
MgO		10.4	10.4	15.0	15.0
CaO		9.1	9.1	9.4	9.4
Na_2O		2.6	2.6	4.8	4.8
K_2O		0.8	.0	.0	.0
Oxygen				150.0	140.0
Total		100.0	94.4		

Column 1	Alkali olivine basalt #4 (Ringwood 1975, p.14)
Column 2	Simplified version of column 1
Column 3	Cation and oxygen proportions for column 2
Column 4	Iron-free version of column 3

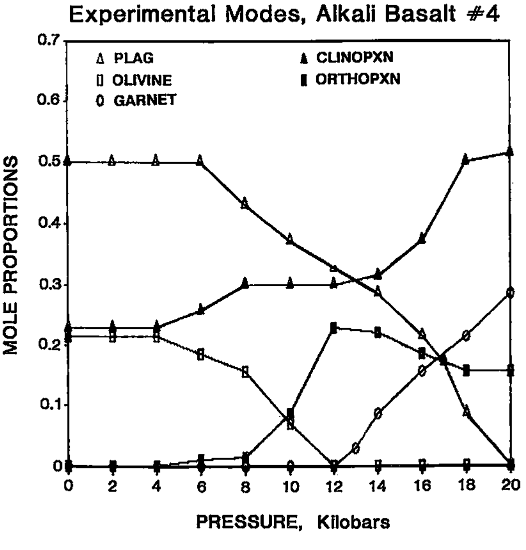

FIG. 11. Variations in modal proportions of minerals in natural alkali basalt at 1100°C, as reported by Green & Ringwood (1967). Composition is given in Table 1, column 1.

basalt reported in the results of high-pressure experiments (Green & Ringwood 1967). The values in Figure 11 have been scaled from an illustration shown by Ringwood (1975, Fig. 1-5), and do not represent, point-for-point, measured values. They show, to the best of our knowledge, the effect of pressure on the modal proportions of phases at 1100°C.

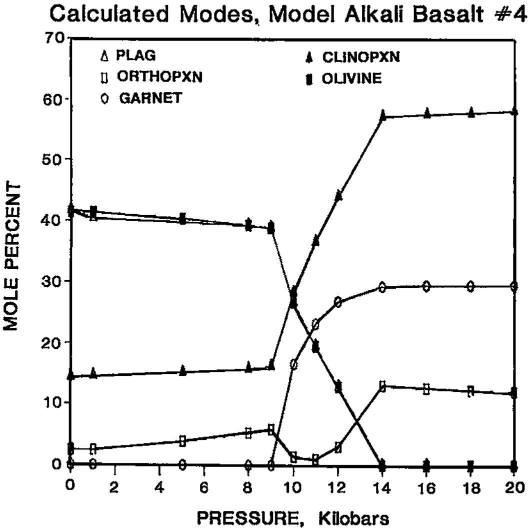

FIG. 12. Computed mineral modes of 'alkali olivine basalt' at 1100°C, similar to that of Figure 11. Composition given in Table 1, columns 2 and 3. Computed with THERIAK (deCapitani & Brown 1987).

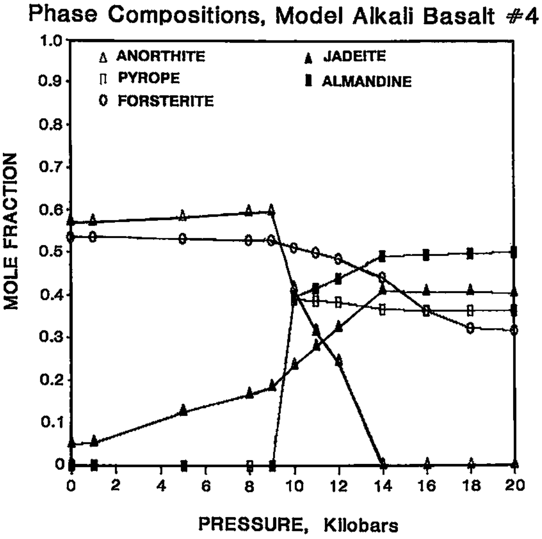

FIG. 13. Computed compositions of phases at 1100°C in the simplified basalt of Table 1, columns 2 and 3. Computed with THERIAK (deCapitani & Brown 1987).

From the experimental work, we may note that the original mode of plagioclase, clinopyroxene, and olivine progressively changes, starting at about 4 kbars, with an increase in clinopyroxene and appearance of orthopyroxene accompanied by a decrease in olivine. At 6 kbars, plagioclase begins to decrease, and at 12 kbars, garnet appears. Beyond this, in the absence of detailed chemical data for the phases, we cannot carry our understanding much further, although we can deduce that the clinopyroxene must become more jadeitic, the plagioclase more sodic, and the garnet more pyropic.

If we turn now to a computed thermodynamic model of the same rock, we may see the same trends. For purposes of this demonstration, I have used a simplified bulk composition shown in Table 1 (columns 2 and 3) in which TiO_2, Fe_2O_3, MnO, and K_2O have been ignored (set to zero). In addition, the model uses only ideal solution-models, although program THERIAK will accept solution models of any complexity. The solutions considered are albite–anorthite, forsterite–fayalite, enstatite–Mg-Tschermaks, diopside–jadeite–Ca-Tschermaks, and almandine–pyrope–grossular. Other phases were treated as stoichiometric compounds. Duhem's theorem dictates that for a particular composition of a system, specification of pressure and temperature will dictate specific values of all activities, phase compositions, and phase proportions. Figure 12 illustrates the variations in phase proportions for the "poor man's alkali basalt" of Table 1, column 3. Figure 12 is the computed model of Figure 11. Some of the differences are undoubtedly due to difficulties in scaling values from the source illustration for Figure 11 (Ringwood 1975), and the others to a combination of simplified composition, simplified solution-models, and inadequacies of the thermodynamic data. Nevertheless, the similarities are striking. Below 9 kbars, phase proportions vary smoothly because with only plagioclase, clinopyroxene, olivine, and orthopyroxene, there are too few phases to fix all chemical potentials. At 9 kbars, garnet appears, the number of degrees of freedom drops to one, and the phase proportions start to change rapidly. At 14 kbars, olivine and plagioclase are gone, and we have an eclogitic mineralogy consisting of garnet, clinopyroxene and orthopyroxene.

The same model predicts the compositions of the phases, which are shown in Figure 13. Notable features include the steady increase of jadeite in clinopyroxene and the abrupt decrease in the anorthite content of plagioclase when garnet first appears. Olivine composition changes smoothly, and over a small range, although its modal proportion goes to zero. These variations in phase composition require parallel variations in the activities of all components, both those that are variable phase-components and those that are only variable system-components. With six components there are six independent chemical potentials or thermodynamic activities, which are shown in Figure 14.

In Figure 14, note first the behavior of the activity of SiO_2. SiO_2 is a system component but not a variable phase-component, its potential being buffered by heterogeneous equilibria among phases containing different amounts of SiO_2. Although quartz is not present, the degree of saturation with respect to β-quartz is defined and readily represented. Anorthite, which is a phase component, has an activity that initially increases slightly with pressure and then drops off rapidly as that component is consumed by reaction. Once plagioclase is completely gone there is still a non-zero activity of the anorthite component. The activities of the garnet components all increase until garnet appears as a phase, at which point pyrope, almandine, and grossular adjust to the changing conditions, with pyrope dropping slightly and almandine and grossular increasing. Kyanite, which never appears as a phase in this bulk composition, shows a steady increase in activity as aluminum is released from plagioclase and incorporated in the pyroxenes.

It is useful to examine another example, similar to the last but lacking iron (Table 1, column 4; Fig. 15). Here we have a 5-component system consisting initially of the four phases clinopyroxene, plagioclase, forsterite and orthopyroxene, with one degree of freedom at any fixed pressure and fixed temperature. With fewer components, there are fewer opportunities to accommodate to a change in pressure and temperature by change in phase compositions, so that the reactions are more abrupt. At 8.6 kbars, garnet appears, forsterite is consumed, plagioclase decreases, and clinopyroxene increases over a pressure range of 500 bars. At 13 kbars, quartz appears, garnet increases again, plagioclase decreases again, and orthopyroxene is entirely consumed. Finally, at 17 kbars, plagioclase is gone, clinopyroxene increases again, garnet decreases slightly, and kyanite appears. These changes imitate a progression from basalt through pyroxene granulite to a quartz-kyanite eclogite, all on the same "basaltic" composition. As with the first model, these modal changes are reflected in the composition of the solid solutions.

Figure 16 illustrates the compositions of plagioclase, garnet, and clinopyroxene for the Fe-free model (Table 1, column 4; Fig. 15). With increasing pressure, the clinopyroxene becomes more jadeitic, the pyrope content of garnet jumps abruptly to 0.8 once garnet appears and, interestingly, the plagioclase responds to every reaction but maintains roughly the same composition until it disappears at 17 kbars. Another side of the same coin may be seen by following the activities of the components.

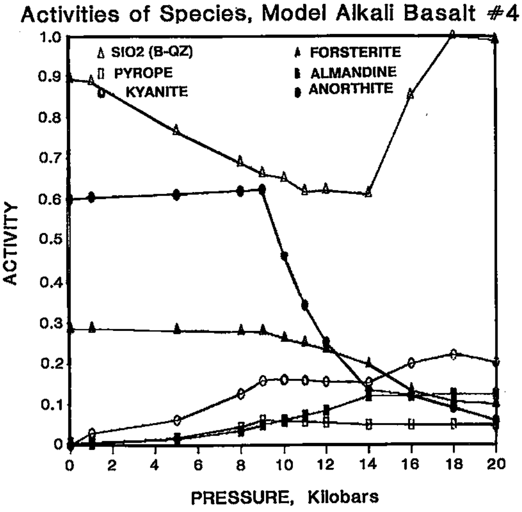

FIG. 14. Computed activities of components at 1100°C in the simplified basalt of Table 1, columns 2 and 3. Computed with THERIAK (deCapitani & Brown 1987).

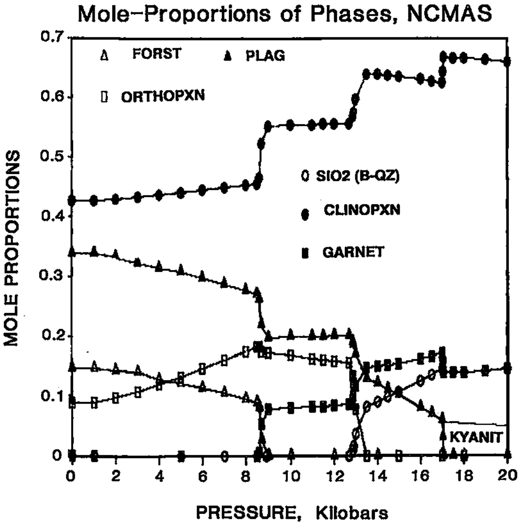

FIG. 15. Modal proportions of phases in an iron-free simulated basalt at 1100°C (Table 1, column 4). Computed with THERIAK (deCapitani & Brown 1987).

Figure 17 shows the variations of component activities for the same system illustrated in Figures 15 and 16. Note how the activity of SiO_2 initially decreases while forsterite is present (activity of Fo $= 1.0$) and then climbs to 1.0 where quartz appears as a phase. Similarly, the activity of pyrope increases until garnet appears (Py 0.55, Gr 0.45) and that of kyanite steadily increases until it appears as a phase. We shall leave this approach to modeling by minimization of free energy with THERIAK (deCapitani & Brown 1987) and project the chemography from albite and quartz, using the method outlined by Greenwood (1975).

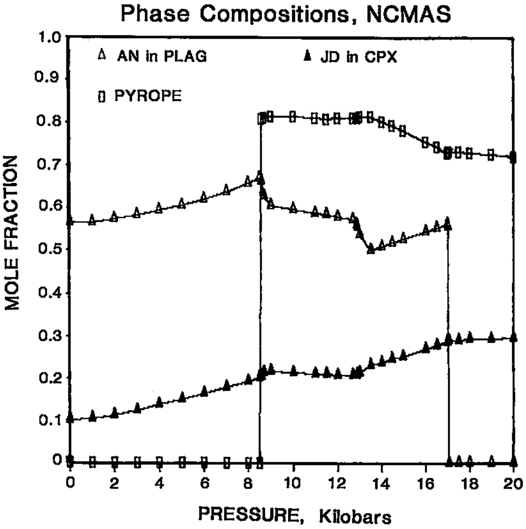

FIG. 16. Compositions of phases in an iron-free simulated basalt at 1100°C (Table 1, column 4).

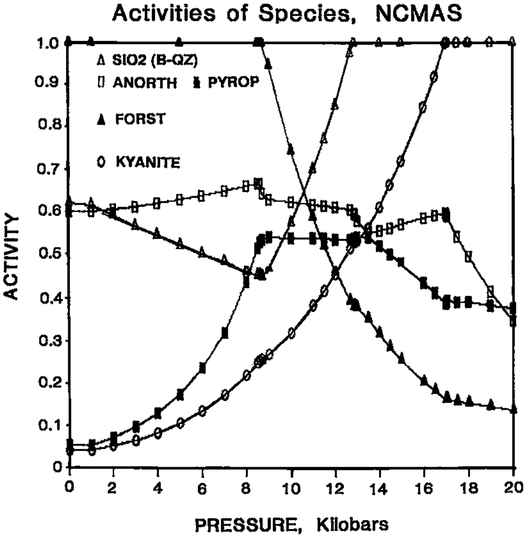

FIG. 17. Activities of components in an iron-free simulated basalt at 1100°C (Table 1, column 4). Computed with THERIAK (deCapitani & Brown 1987).

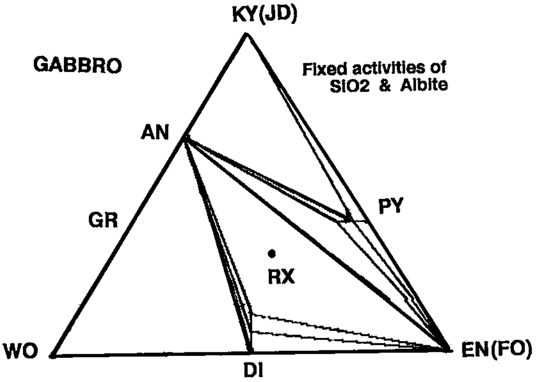

FIG. 18. Chemographic diagram of the system NCMAS projected from albite and quartz at 1 bar, 1100°C.

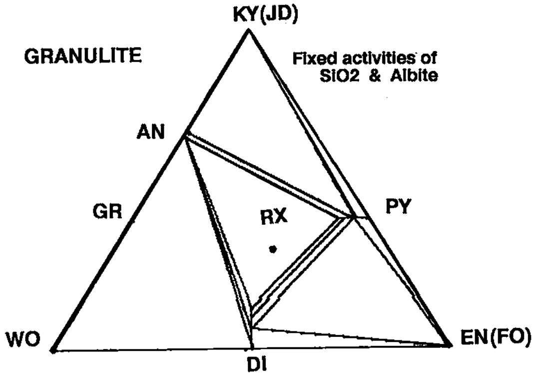

FIG. 19. Chemographic diagram of the system NCMAS projected from albite and quartz at 14 kilobars, 1100°C.

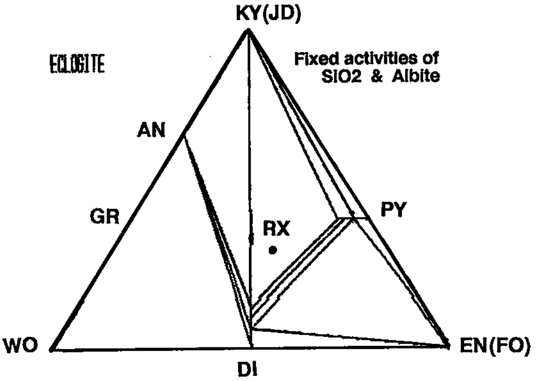

FIG. 20. Chemographic diagram of the system NCMAS projected from albite and quartz at 18 kilobars, 1100°C.

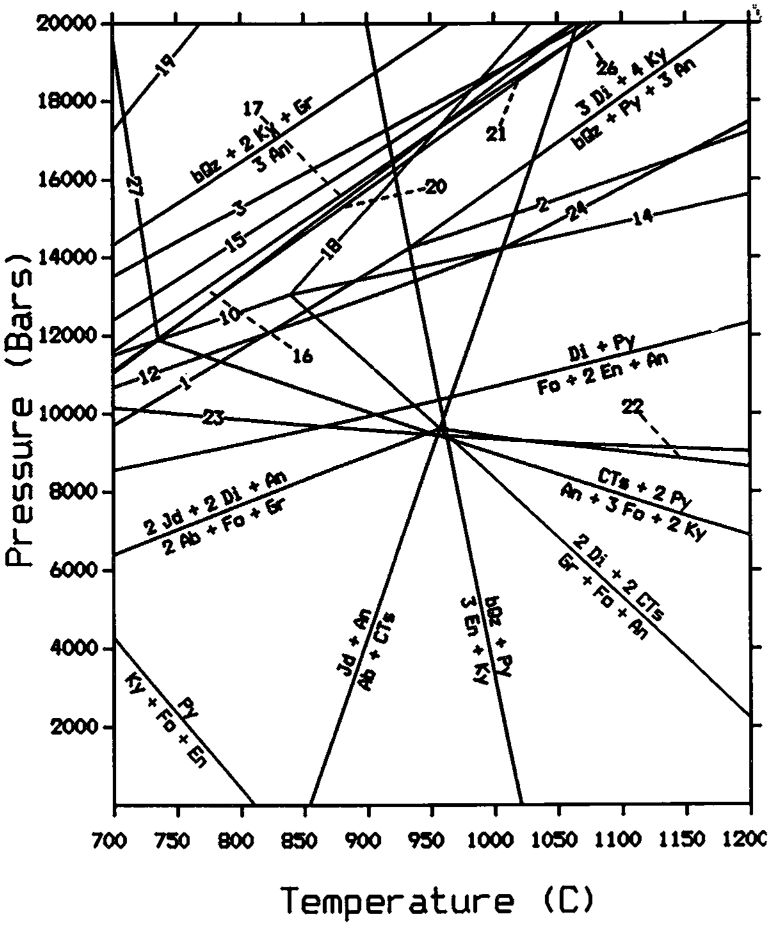

FIG. 21. *P–T* projection of the stable stoichiometric equilibria in the NCMAS system. Computed with GEOCALC (Brown *et al.* 1988) using the data of Berman (1988). The reactions are listed below with the reactant assemblages (LHS) stable on the high-pressure side of the curve: 1) Di + Ky = En + An, 2) bQz + Py + Di = An + 4En, 3) Jd + 2En = Ab + Fo, 4) Di + Py = Fo + 2En + An, 5) bQz + 2Ky + Gr = 3An, 6) Jd + An = Ab + CTs, 7) bQz + Py = 3En + Ky, 8) 3Di + 4Ky = bQz + Py + 3 An, 9) 2Jd + 2Di + An = 2 Ab + Fo + Gr, 10) Gr + 2Py = 3Fo + 3 An, 11) 2Di + 2CTs = Gr + Fo + An, 12) Py + Jd + Di = Ab + An + 2Fo, 13) Py = Ky + Fo + En, 14) CTs + Py + Di = 2An + 2Fo, 15) Ab + Gr + 2Ky = Jd + 3An, 16) 6Ky + Gr + 3Di = 6An + Py, 17) Gr + 2Ky = CTs + 2An, 18) Py + 2Gr = 3Di + 3CTs, 19) Ky + Jd + 3En = Ab + Py, 20) 4Ky + Jd + 3Di = Ab + 3An + Py, 21) CTs + 4Ky + 3Di = 4An + Py, 22) CTs + Jd + 2Di = Ab + Fo + Gr, 23) 2Py + Jd = Ab + 3Fo + 2Ky, 24) Py + 2Jd + Di = 2Ab + 2Fo + CTs, 25) CTs + 2Py = An + 3Fo + 2Ky, 26) 3Di + 4Jd + 4Ky = 3CTs + Py + 4Ab, and 27) 3CTs + 4Py = 6Fo + Gr + 6Py.

The results are shown in Figures 18, 19, and 20, in which each projection requires that the activities of albite and quartz be uniform in every 3-phase field. The assumption of uniform activity of albite is roughly valid even between diagrams, as may be seen from Figure 17, but the assumption of constant activity of SiO_2 is valid only over each individual projection. Besides the phase compositions, the composition of the bulk system is shown as "RX", the "poor man's basalt" of Table 1 (column 4). In Figure 18 we see the "rock" at one bar, being made up of plagioclase, diopsidic clinopyroxene, forsterite, and enstatite (forsterite and enstatite coincide in this projection). Garnet and

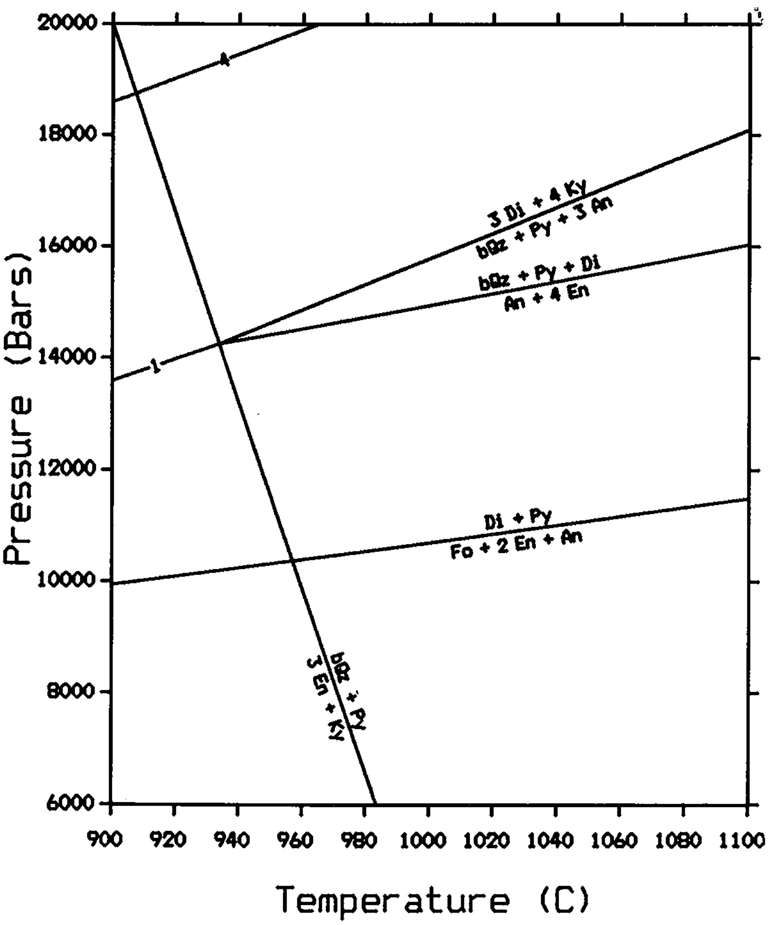

FIG. 22. *P–T* projection of the stable stoichiometric equilibria in the CMAS system. Computed with GEOCALC (Brown *et al.* 1988) using the data of Berman (1988). The numbered reactions (without labels) are listed below with the reactant assemblages (LHS) stable on the high-pressure side of the curve: 1) Di + Ky = En + An, and 4) bQz + 2Ky + Gr = 3 An.

kyanite are both stable, but not in this bulk composition. In Figure 19, drawn for 14 kbars, we see a granulite mineralogy of plagioclase, clinopyroxene, garnet, and quartz (not shown owing to projection). Olivine and orthopyroxene have gone, and kyanite has not yet appeared. Finally, in Figure 20, drawn for 18 kbars, plagioclase has gone, kyanite has appeared, and the clinopyroxene has become more aluminous (jadeitic), resulting in a quartz–kyanite eclogite. For yet another view of this same system, we may model it in terms of the full set of stable and metastable reactions that are possible among all the end members of the phases under consideration, and represent the results in a pressure–temperature (*P–T*) diagram. This phase of our modeling can best be done with a set of programs encompassed by "GEOCALC", (Brown *et al.* 1988), using the database of Berman (1988).

Figure 21 is a *P–T* projection of the stable equilibria in the system NCMAS, which contains all the components and phases represented in Figures 15 through 20. Comparison of Figures 15 and 21 will show that the reactions most affecting the mode are to be found in the subsystem CMAS, and this much simpler system is shown in Figure 22. Figure 22 is calculated for the stable equilibria among stoichiometric phases of CMAS, but our model system contains solid solutions. Therefore, we must use activities appropriate to the equilibrium condition of our assemblage. At each pressure, the activities are defined, so that no one set of activities can be used for an entire *P–T* projection.

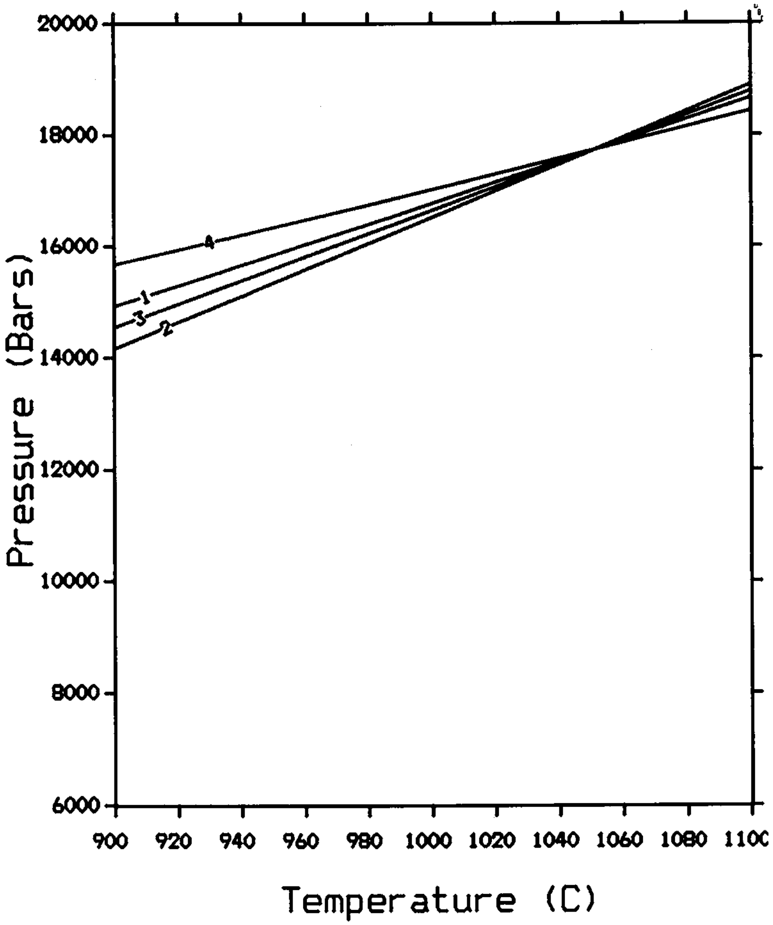

FIG. 23. P–T projection of the stable stoichiometric equilibria in the CMAS system. Computed with GE0CALC (Brown *et al.* 1988) using the data of Berman (1988). The numbered reactions (without labels) are listed below with the reactant assemblages (LHS) stable on the high-pressure side of the curve: 1) bQz + 2Ky + Gr = 3An, 2) 3Di + 4Ky = bQz + Py + 3An, 3) 3Di + Gr + 6Ky = Py + 6An, and 4) 3bQz + Py + 2Gr = 3An + 3Di.

Geothermobarometry in this system would generally be approached by analyzing the phases of an assemblage, applying an appropriate solution-model (optimistically), calculating the activities of the reacting phase-components, and then computing the positions of the effective equilibria as displaced by these activities. In Figure 23 are plotted four of the equilibria in the system, using activities of components derived for a pressure of 17 kbars and 1055°C. The four curves all pass through the same P–T point, a feature guaranteed in this example by the fact that an internally consistent set of data was used together with activities that were dictated by the same data and minimized free energy at the same pressure and temperature. In a real attempt at geothermobarometry, one would have uncertainty in the activities introduced by analytical error, by inadequate solid-solution models, and by imperfect equilibration among the minerals of the rock under study. When multiple equilibria of this sort fail to pass through a single point in a real attempt at barometry using an internally consistent data-set, one is forced to turn to analytical error and imperfect equilibrium in the attempt to rationalize the results. Perhaps it should be noted, however, that an incorrect but thermodynamically consistent data-set will give a perfect intersection that passes through the wrong coordinates.

For yet another view of this simplified basalt–eclogite transition, Figure 24 shows a P–T projection giving the first appearance of garnet and the dis-

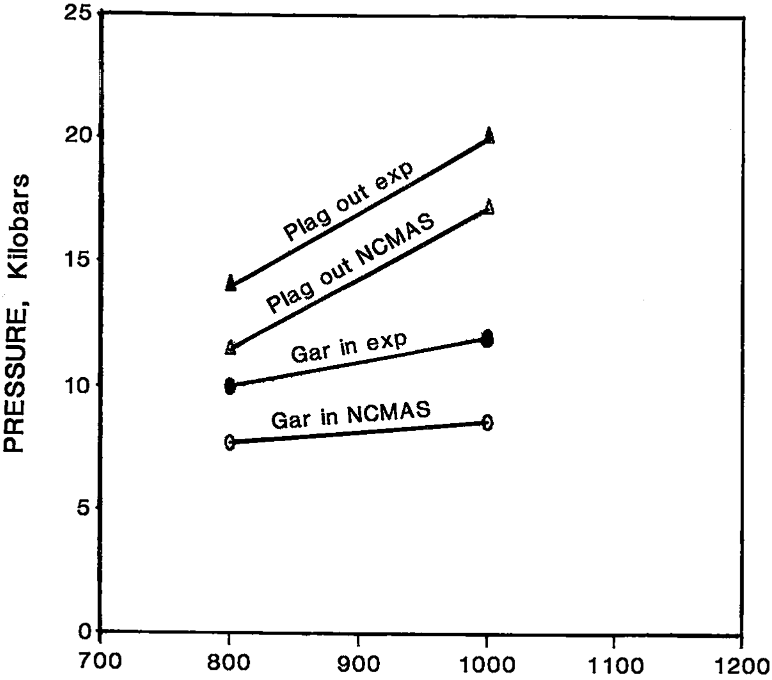

FIG. 24. *P–T* projection of the first appearance of garnet and the disappearance of plagioclase in alkali olivine basalt (Table 1, column 1), after Green & Ringwood (1967), and in simplified basalt (Table 1, column 3). Incoming of garnet with increasing pressure shown with circles (filled: experimental, open: calculated). Disappearance of plagioclase with increasing pressure is shown with triangles (filled: experimental, open: calculated).

appearance of plagioclase in alkali basalt #4 (Ringwood 1975; Table 1, column 4) on the same diagram with the same changes in the Fe-free NCMAS system (Table 1, column 3). This model system brings garnet into the assemblage about 2 kbars lower than the experiments, and eliminates plagioclase about 3 kbars lower than the experiments. The correspondence among all these approaches suggests that we are now in a good position to begin serious modeling of such systems and to begin the process of thinking, and modeling, and testing a number of assumptions about equilibrium and solution models. In particular, the availability of such thorough procedures of modeling will facilitate the design of experiments and the interpretation of experimental results in much more complex systems than could previously be considered with any real degree of rigor.

CONCLUSIONS

I have presented an outline of what I believe to be characteristics for which we should strive in modeling geological, and especially petrological, problems, and have used a thermodynamic example by way of illustration. The thermodynamic model has the following properties, which in my opinion should be characteristics of any 'model' of earth processes:

A guiding conceptual model
Theoretically based or rigorous submodel
Predictive capability
Testable predictions

Alas, not all of our science has so mature a model as the thermodynamic one. I urge that we all strive to draw the line between vague, 'cloud-9' scenarios and serious models, and to use the word 'model' only for logical propositions, not necessarily mathematical, that have *necessary, testable consequences.* Let us not grace loose thinking with the word 'model'.

"Model" starts where "scenario" ends (Fig. 25).

ACKNOWLEDGEMENTS

As noted in the introduction, I am indebted to many students and colleagues, not for reading this

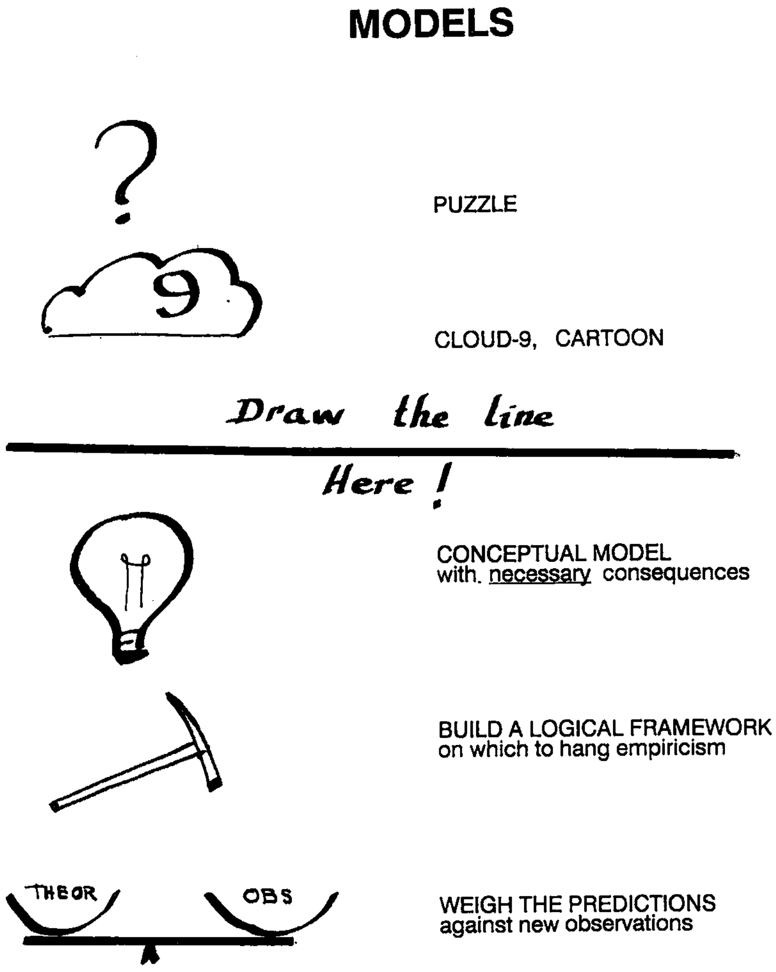

FIG. 25. Cartoon to emphasize a prejudice that the word 'model' should be reserved for carefully conceived logical hypotheses that have testable consequences.

manuscript, a labor I could not ask, but for continued inspiration in matters scientific. Most especially, I am indebted to my colleague Tom Brown, and to Terry Gordon, Martin Engi, Rob Berman, "Capi" deCapitani, and Lee Pigage, for their many rejections of my fuzzy thinking and for their innovative and varied approaches to petrology.

REFERENCES

BERMAN, R.G. (1988): Internally consistent data base for minerals in the system Na_2O-K_2O-CaO-MgO-FeO-Fe_2O_3-Al_2O_3-SiO_2-TiO_2-H_2O-CO_2. *J. Petrol.* **29**, 445-522.

______, BROWN, T.H. & GREENWOOD, H.J. (1985): An internally consistent data base for minerals in the system Na_2O-K_2O-CaO-MgO-FeO-Fe_2O_3-Al_2O_3-SiO_2-TiO_2-H_2O-CO_2. *Atomic Energy of Canada Ltd., Techn. Rec. TR-377.* (Doc. Distr. Office, Chalk River, Ontario K0J 1J0).

BROWN, T.H., BERMAN, R.G., and PERKINS, E.H. (1988): Ge0-Calc: Software package for calculation and display of pressure-temperature-composition phase diagrams using an IBM or compatible personal computer. *Comput. & Geosci.* **14**, 279-289.

DECAPITANI, C. & BROWN, T.H. (1987): The computation of chemical equilibrium in complex systems containing non-ideal solid solutions. *Geochim. Cosmochim. Acta* **51**, 2639-2652.

GIBBS, J.W. (1876): On the equilibrium of heterogeneous substances. *Trans. Conn. Acad.* **III**, 108-248.

GREEN, D.H. & RINGWOOD, A.E. (1967): An experimental investigation of the gabbro to eclogite transformation and its petrological applications. *Geochim. Cosmochim. Acta* **31**, 767-833.

GREENWOOD, H.J. (1975): Thermodynamically valid projections of extensive phase relations. *Am. Mineral.* **60**, 1-8.

PERKINS, E.H., BROWN, T.H. & BERMAN, R.G. (1986): Three programs which calculate pressure-temperature-composition diagrams. *Comput. & Geosci.* **12**, 749-755.

RINGWOOD, A.E. (1975): *Composition and Petrology of the Earth's Mantle*. McGraw-Hill, New York.

Received January 4, 1989.